# LATERAL VARIATIONS IN LOWER MANTLE SEISMIC VELOCITY

Thomas S. DUFFY and Thomas J. AHRENS

*Seismological Laboratory, California Institute of Technology, Pasadena, CA 91125, USA*

**Abstract.** An important finding of recent tomographic studies is that the lower mantle, at a constant radius, has RMS variations of P- and S-wave velocity of ~0.1–0.2% and ~0.2–0.4% from average Earth models and these lateral variations correlate spatially. Both tomographic and free oscillation studies suggest that the magnitude of relative shear velocity variations is at least twice as large as the magnitude of relative compressional velocity variations. This result can be expressed as: $\nu = (\partial \ln V_S / \partial \ln V_P)_P > 2$. In contrast, laboratory studies near ambient pressure have consistently found that the ratio of relative shear velocity variations to relative compressional velocity variations is near unity for metals and minerals generally, and mantle minerals, in particular. Laboratory studies further suggest, although not yet conclusively, that $\nu$ is not strongly pressure or temperature sensitive. In this paper, we seek to determine whether high observed values of $\nu$ can be explained by the presence of 0.1–2.0% volatile-rich partial melt heterogeneously distributed in the lower mantle. The $H_2O$ budget of the lower mantle is estimated to be 0.1–0.3 wt.% based on the present $^3He$ flux, equation of state data for hydrous minerals, and shock devolatilization experiments which define a maximum radius of the Earth's primitive accretion core. The effect of hydrous melts on $\nu$ is calculated using theories for the elastic properties of a two phase aggregate. Results indicate that, depending on aspect ratio and geometry, 0.1–2% partial melting in conjunction with ~100 K thermal anomalies can explain the seismic result so long as the compressibility of the melt differs by less than about 20% from the surrounding solid. On this basis, we conclude that small amounts of water-rich partial melt are a possible explanation for the large values of $(\partial \ln V_S / \partial \ln V_P)_P$ observed for the lower mantle.

## Introduction

Seismic tomography yields three-dimensional global images of mantle structure. A number of images have been constructed using both body waves and surface waves (e.g., Nataf *et al.*, 1984, 1986; Dziewonski, 1984; Hager and Clayton, 1989; Tanimoto, 1990; Davies, 1990; Inoue *et al.*, 1990). An important feature of these results involves the relative variation of seismic velocities. The relative variation of compressional wave velocity, $V_P$, and shear wave velocity, $V_S$, from a radially averaged model at a given position in the Earth can be described by the parameter $\nu$

$$\nu = \left( \frac{\partial \ln V_S}{\partial \ln V_P} \right)_P \qquad (1)$$

The value of $\nu$ obtained from comparing P- and S-wave velocity models in the lower mantle is 2–2.5 (Dziewonski and Woodhouse, 1987). That is, relative anomalies of shear wave velocity are twice as large as relative compressional wave velocity anomalies in the lower mantle. Davies (1990), in an inversion of teleseismic P- and S-wave data, obtained $\nu \approx 2$ for the globally averaged lower mantle although values greater than 4 were obtained in some regions. Tomographic studies may suffer from biases related to parameterization or noise (Romanowicz, 1991). Free oscillation splitting functions are also sensitive to $(\partial \ln V_S / \partial \ln V_P)_P$. Li *et al.* (1991) used this data to constrain $\nu$ to lie between 1.7 and 2.6 with 75% confidence and with an optimal value of 2.3. In contrast, in a study of global long-period PcP-P and ScS-S arrival times, Pulver and Masters (1990) obtained a lower value for $\nu$ of 1.7.

One assumption which can be reasonably made as giving rise to the simultaneous deviation above and below the average value for P and S velocity is that these are due to the effect of variation in temperatures, possibly arising from mantle convection. At pressures of the deep lower mantle at depths of 2300 km, and hence, pressure in the range of ~100 GPa the observed RMS deviations of seismic velocity from the average are about ~0.1–0.2% and ~0.2–0.4% for P- and S-wave velocity over length scales of ~$10^3$ km. Recently, Duffy and Ahrens (1991b) inferred that the temperature variations which could give rise to the seismic velocity anomalies in the lowermost mantle were on the order of 120 ± 100 K.

As shown in Fig. 1, laboratory determinations of $(\partial \ln V_S / \partial \ln V_P)_P$ at ambient pressure range from 0.7 to 1.4 for mantle minerals (Sumino and Anderson, 1984). The discrepancy between the seismological results and the laboratory data has been ascribed to a number of factors including the effects of pressure, temperature, composition, and phase. Anderson (1987) proposed that the observed $\nu$ values are intrinsic to the high pressure-high temperature environment of the Earth's interior. Attempts to verify this result using potential models for minerals have reached conflicting conclusions (Reynard and Price, 1990; Agnon and Bukowinski, 1990). At ambient pressure, $\nu$ does not change significantly up to ~1700 K (Isaak *et al.*, 1989). The application of pressure alone has not been found to have a significant effect on this quantity (Graham and Hilbert, 1988).

Sound velocities at high pressure have been measured under shock conditions for a number of metals. These data, in combination with finite strain extrapolations of low pressure data, allow inferences to be drawn regarding the effects of temperature on wave velocity at high pressure (Duffy and



*High-Pressure Research: Application to Earth and Planetary Sciences*, edited by Y Syono and M H Manghnani, pp 197 – 205

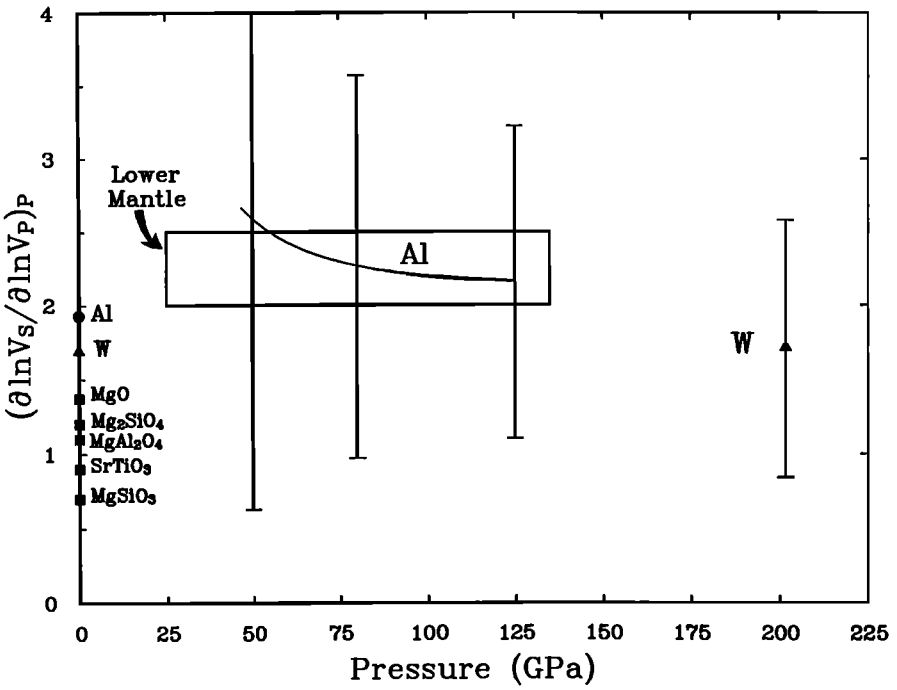


Figure 1. The parameter $(\partial \ln V_S/\partial \ln V_P)_P$ as a function of pressure. Lower mantle values from seismic tomography are indicated by the box. Zero pressure values for minerals are shown as solid squares. Zero pressure values for aluminum (Al) and tungsten (W) are shown by the filled circle and triangle, respectively. High pressure-high temperature values from shock data for aluminum between 50 and 125 GPa are shown by the solid line and for tungsten at 202 GPa by the triangle. For Al, representative error bars at selected pressures are shown.

Ahrens, 1991b). Compressional and bulk wave velocities along the Hugoniot to 125 GPa in aluminum and at 202 GPa for tungsten were analyzed for their relative variations. In aluminum, calculated Hugoniot temperatures at pressures between 50 and 125 GPa range from 1000–5100 K and the estimated temperature in tungsten at 202 GPa is 3600 K. High pressure value of $\nu$ can be obtained from compressional and bulk sound speeds using:

$$\nu = \frac{V_P^2 - V_P V_B \dot{V}_B / \dot{V}_P}{V_P^2 - V_B^2} \tag{2}$$

where $V_B$ is the bulk sound velocity and $\dot{V}_S$ and $\dot{V}_P$ are the temperature derivatives of the bulk and compressional sound velocities, respectively. Temperature derivatives were obtained by differencing Hugoniot and adiabat velocities and dividing by the calculated temperature difference at a given pressure (Duffy and Ahrens, 1991b). The results are displayed in Fig. 1 and show that $\nu$ values at pressures between 50 and 125 GPa for Al and at 202 GPa for W are similar to the zero pressure $\nu$ values for these materials, although the uncertainties are large due to uncertainties in the calculated temperature derivatives.

The experimentally determined values of $\nu$ at high pressure and/or high temperature do not significantly differ from zero pressure values, although available data are too limited to conclusively reject a strong pressure/temperature dependence of this quantity in geological materials. The experimental determinations are sufficiently suggestive, however, that we feel it is worthwhile to consider other possible explanations for the seismically observed phenomena.

From the Earth's average radial structure, the ratio of $V_P$ to $V_S$ is constrained to be 1.8 to 1.9 in the lower mantle. Eq. (1) can be written as

$$\nu = \left(\frac{\partial \ln V_S}{\partial \ln V_P}\right)_P = \frac{V_P}{V_S}\frac{(\partial V_S/\partial T)_P}{(\partial V_P/\partial T)_P} = \frac{V_P}{V_S}\frac{\dot{V}_S}{\dot{V}_P} \tag{3}$$

For $\nu$ between 1.7 and 2.5, we must have $\dot{V}_S/\dot{V}_P = 0.9$ to 1.4 in the lower mantle. This means that the temperature coefficient of the shear velocity must be nearly equal to or greater than the temperature coefficient of the compressional velocity for lower mantle material. Of the wide range of compositions and structures contained in the elasticity compilations of Sumino and Anderson (1984) and Simmons and Wang (1971), there are only two materials ($Hg_2Cl_2$ and

$NH_4Al(SO_2)_3 \cdot 12H_2O$) for which $\dot{V}_S$ is unambiguously larger than $\dot{V}_P$. Thus, the required condition is rare at ambient pressure. However, the rocksalt-structure oxides have one of the highest ratios of $\dot{V}_S/\dot{V}_P$ for any structure. In the case of MgO, $\dot{V}_S/\dot{V}_P$ is 0.8. Yeganeh-Haeri and Weidner (1989) have suggested that the temperature derivative of the shear modulus of silicate perovskite may need to be anomalously large for the shear velocity of this material at high pressure to be consistent with lower mantle shear velocities. Shear mode softening due to the proximity of a phase transition under lower mantle conditions is a potential explanation for this (Yeganeh-Haeri and Weidner, 1989). Alternatively, a high FeO content in the lower mantle might reconcile the ambient pressure shear moduli of perovskite and magnesiowustite to lower mantle values. Changes in chemistry can also cause changes in $\nu$ although the effect is limited. For example, at ambient conditions, a change in composition from $(Mg_{0.9}Fe_{0.1})_2SiO_4$ to $(Mg_{0.7}Fe_{0.3})_2SiO_4$ produces a $\nu$ value of 1.4 if no temperature effect is present.

To obtain a theoretical model which provides a rationale for the high observed values of $\nu$, we examine the effect of 0.1 to 2% partially molten material in various geometries which we imagine is heterogeneously dispersed in the lower mantle. We assume that this heterogeneously distributed lower mantle melt which we also infer is rich in volatiles (e.g., $H_2O$ and $CO_2$) could be present from two sources: the subduction to great depth of $H_2O$- and $CO_2$-rich oceanic lithosphere or primordial (e.g. a vestige of the accretion of the Earth). We examine several lines of evidence to constrain the maximum water content of the lower mantle. Although other volatiles beside $H_2O$ (e.g. $CO_2$, CO) are possible constituents of the lower mantle, we restrict our attention to $H_2O$ because, at least in the crust and upper mantle, it appears to be by far the most abundant volatile species.

## The Partial Melt Hypothesis

In the upper mantle, large variations in shear velocity relative to compressional velocity has long been interpreted as a consequence of partial melting (Anderson and Sammis, 1970). Here we consider the possibility that partial melting in the lower mantle can explain the anomalous seismic observations discussed above. In the case where velocity variations are solely due to changes in rigidity, the relative velocity variation is (Anderson, 1987; Davies, 1990):

$$\nu = \frac{3V_P^2}{4V_S^2} \tag{4}$$

For the lower mantle, $V_P/V_S \approx 1.8$, yielding $\nu \approx 2.4$. Thus, partial melting or other phenomena which dominantly affect the rigidity are consistent with the seismic results, at least to first order. A more detailed consideration of the partial melt hypothesis requires consideration of the properties of a two phase medium as well as the effect of changes in other properties and thermal effects. A series of simple mixing calculations was undertaken to determine if the above result holds under plausible lower mantle conditions.

Our approach is to assume that thermal, rather than compositional, anomalies exist throughout the lower mantle and give rise to the velocity anomalies observed by tomographic studies. The magnitude of these anomalies is less than 220 K based on the magnitude of P-velocity variations and high-pressure values of $(\partial V_P/\partial T)_P$ from shock studies (Duffy and Ahrens, 1991b). These anomalies are then assumed to cause varying amounts of partial melt throughout the lower mantle. Lower mantle temperatures are estimated to lie between 2000–3000 K, at least several hundred K below the solidus of perovskite, the probable main lower mantle constituent (Jeanloz and Morris, 1988). The presence of small quantities of water-bearing phases in the lower mantle, however, may provide a low melting point fraction. At upper mantle pressures, the presence of small amounts of water lowers the solidus by several hundred K (Green and Liebermann, 1976; Wyllie, 1982).

Little is known about the stability of hydrous minerals under lower mantle conditions. A number of dense, water-bearing silicates have been identified under upper mantle conditions (Ringwood and Major, 1967; Finger and Prewitt, 1989; Ahrens, 1989; Kanzaki, 1991). The hydrous mineral phase D (also known as phase D') of inferred composition $MgSiO_3 \cdot H_2O$ has now been identified under lower mantle conditions in diamond cell experiments (Liu, 1987; Li and Jeanloz, 1991). $H_2O$ in the mantle may be a remnant from the earliest stages of accretion (Ahrens, 1989; Ahrens, 1990) or could be delivered from the hydrosphere via subduction (Ito *et al.*, 1983; Peacock, 1990). Estimates of mantle water content based on accretion and petrological models range from 0.1–0.3% (Ringwood, 1975; Abe and Matsui, 1986; Liu, 1987). In the next section, we obtain estimates of lower mantle water content using new geophysical data.

## Bounds on the Water Content of the Lower Mantle

Three lines of evidence may be used to place upper bounds on the water content of the lower mantle. (1) Application of shock wave devolatilization studies to define the primitive accretion core (PAC) of the Earth. (2) A comparison of lower mantle pressure-density profiles with shock wave equation of state data for serpentine and brucite, and (3) application of the $^3He$ flux from the Earth as a guide to the amount of undegassed mantle and core material in the Earth.

(1) Serpentine is taken to be representative of the phyllosilicates and thus contains most of the water carried by objects such as the primitive meteorites (e.g., C1 chondrites)

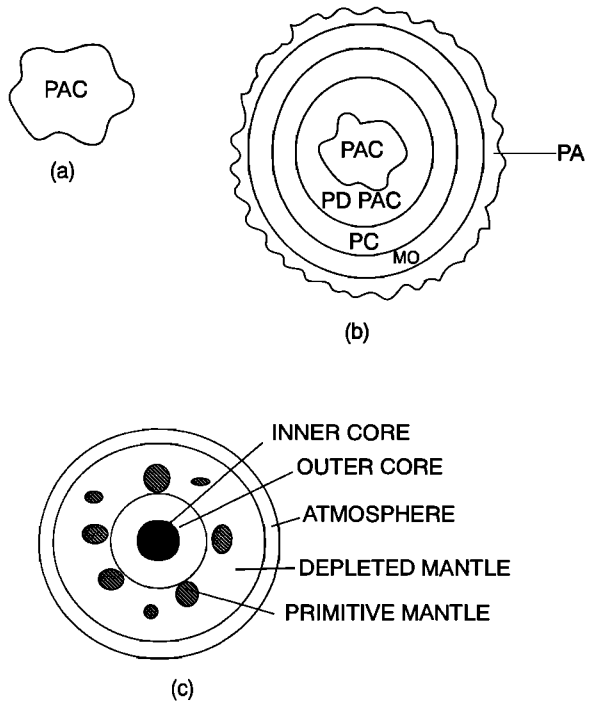


Figure 2. Diagrammatic sketch of the three phases of Earth accretion. a) Formation of a primitive accretion core (PAC). This is a ~800 km radius proto-Earth for which the infall velocity is so low (≤0.5 km/s) that virtually no impact volatilization occurred. Subsequent accretion does incur partial volatile loss from infalling planetesimals. b) A very idealized proto-Earth when it has substantially accreted but before substantial core segregation and core infall has taken place. The PAC is surrounded by a partially devolatilized primitive accretion core (PDPAC), that in turn is surrounded by a partially segregated primitive liquid core (PC) which in turn is surrounded by a magma ocean (MO) which is covered with a massive proto-atmosphere (PA) (after Ahrens, 1990). c) The Earth today. Fragments of primitive mantle, derived from the PAC are shown, distributed in the mantle but preferentially lying in the lower mantle (after Davies, 1981).

which in turn are taken to be a model of the planetesimals which gravitationally accreted to form the Earth. Impact devolatilization experiments conducted on serpentine (Lange and Ahrens, 1982; Tyburczy *et al.*, 1990) provide a basis for defining the size of the growing Earth at which point infalling planetesimals impact the planet with sufficient velocity that high enough shock pressures (~5 GPa) are generated within the planetesimals that devolatilization of $H_2O$ (into a primitive atmosphere) begins. This occurs when the growing planet is about 0.12 of its final radius, or ~800 km. Material within this radius, we define as the primitive accretion core (PAC), (Fig. 2a). Presumably none of this material has suffered substantial impact devolatilization. Upon further accretion and impact of successive planetesimals, the growing Earth become increasingly shock devolatilized. When the Earth accreted to a radius of ~0.32 of the final radius, or $2 \times 10^3$ km, which we define as partially devolatilized primitive accretion core (PDPAC), we assume all of the planetesimal impacts are devolatilized. Further accretion leads to formation of a magma ocean and a proto-core and the initial planet (Fig. 2b) is surrounded by a primitive atmosphere which thermally blankets and traps the impacting energy (Abe and Matsui, 1986). Following the ideas of Stevenson (1981), Anderson (1989), and Ahrens (1990), the unstably layered assemblage is expected to overturn and result in the internal structure present today. Although the undegassed fragments of the PAC are later stirred into the mantle via thermal convection (e.g. Davies, 1981), we presume below that this material accounts also for $^3He$ flux. The mass in the PAC and PDPAC are estimated using the results of the shock devolatilization experiments as $1 \times 10^{25}$ and $4.5 \times 10^{25}$ grams, respectively. We assume that the planetesimals which form the Earth had a water content comparable to the most water-rich carbonaceous chondrites e.g., Orgueil (Wiik, 1956), which is ~0.2 (mass fraction). Anders (personal communication, 1990) has argued that based on the depletion of other volatile species in the Earth, the Earth must have formed from less than 1.6% hydrated planetesimals. However, the upper mantle and crust may have formed from primordial material which was more depleted in volatiles than C1 chondrites. The higher value of $H_2O$ content implies that the maximum initial internal water content of the Earth was $2 \times 10^{24}$ g in the PAC and $9 \times 10^{24}$ g in the PDPAC. The values correspond to 1.5 and 6.5, or a total of 8 (±5) present ocean equivalents of internal water, or 0.28% by mass of the mantle. If we assume that 50% of the mantle has outgassed over geologic time (Allègre *et al.*, 1987) and there is no significant return of $H_2O$ from subduction, then the water content of the present mantle would be less than 0.14%.

(2) Recent shock wave equation of state measurements for brucite ($Mg(OH)_2$) (Duffy *et al.*, 1991a) and serpentine ($Mg_4Si_2O_5(OH)_4$) (Tyburczy *et al.*, 1991) when temperature-corrected to lower mantle geothermal conditions provide upper bounds on the high pressure phase assemblage's water content. In the case of brucite, the lower mantle density-pressure data can be fit with an assemblage of $(Mg_{0.85}Fe_{0.15})SiO_3$ (perovskite) plus $(Mg_{0.85}Fe_{0.15})(OH)_2$, where the latter phase can comprise up to 10% (by mass) of the lower mantle defined by the PREM model (Dziewonski and Anderson, 1981). This would then yield a maximum lower mantle water content of some 3%. Similarly, if the high pressure phase(s) assemblage of serpentine is assumed to be representative of the actual lower mantle water bearing phase, with a (Mg+Fe)/Si atomic ratio of 1.5, then a mantle with Mg/(Mg+Fe) of 0.80 and 2% (by mass) $H_2O$ was found to fit the density-pressure PREM lower mantle.

(3) The flux of $^3He$ (which is completely non-radiogenic and hence primordial) from the Earth has been assumed to have its source in the fraction of the Earth's interior which

has not been completely degassed. The mass of this reservoir may be conservatively estimated by assuming its radius, $r_1$, is related to the $^3$He flux, $F$, over geologic time, $T_e$, the surface area of the Earth, $A_e$, the mean Earth density, $\rho_e$, the He content of $C_1$ chondrites, $X_{He}$, the ($^3$He/$^4$He) ratio of $C_1$ chondrites and, $A$, Avogadro's number, by:

$$FA_e = A\left(\frac{4}{3}\pi r_1^3\right)\rho_e X_{He}\left(^3\mathrm{He}/^4\mathrm{He}\right)/T_e \qquad (5)$$

When we assume $F = 3$ atoms/(cm$^2$ sec) (Welham and Craig, 1983), $\rho_e = 5.52$ g/cm$^3$, $X_{He} = 2.26 \times 10^{-9}$ mole/g, and $^3$He/$^4$He $= 1.42 \times 10^{-4}$ (Ander and Ebihara, 1982) Eq. (5) yields: $r_1 \approx 800$ km, or for a uniform Earth, a mass fraction of undepleted material of 0.002. If this mass fraction is related to a water-rich model planetesimal material such as the Orgueil meteorite which has 0.2 mass fraction water, the $^3$He reservoir could be associated with 1.7 oceans of waters in the Earth's interior or, if distributed largely in the lower mantle, this would yield 0.08% $H_2O$. Upon comparing the three upper bounds on the water content of the lower mantle, we believe that the bounds obtained from accretion considerations (Method 1) and from the $^3$He flux (Method 3) are most credible. These agree within a factor of 3.5. Method 2 is certainly valid, but it is a permissive bound whereas, we believe the physical constraints of the 0.28% and 0.08% bounds from accretion and $^3$He production are obtained via more persuasive arguments.

## Seismic Velocity of a Lower Mantle Containing Small Quantities of Partial Melt

The effect of partially molten hydrous phases on seismic properties can be determined using theories for the elastic properties of a multiphase aggregate. Thus, we tacitly assume that what water is present in the lower mantle will, in analogy to the behavior of upper mantle assemblages, both strongly control the amount of partial melt and be preferentially partitioned into the melt phase. It has recently been demonstrated that water is soluble in silicate melts at lower mantle pressures and temperatures (Williams, 1990). In order to treat the case of a partially molten rock, information about the geometry of the melt fraction must be included. Three different geometries for the melt fraction were considered here: sphere, tube, and disk. For tube- and sphere-shaped melt inclusions, the self-consistent scheme (SCS) described by Watt *et al.* (1976) was used. In this method, the effect of interactions between the inclusions is approximately taken into account and the aspect ratio of the inclusions is fixed. A general expression for the effective bulk and shear moduli in the SCS approach is

$$\frac{M^* - M_1}{M_2 - M_1} = v_2\left(1 + \frac{v_1(M_2 - M_1)}{M_1 + F}\right)^{-1} \qquad (6)$$

where $M$ is either the bulk or shear modulus, $M^*$ is the effective modulus of the aggregate, $v$ is the volume fraction of each component, and the subscript 1 refers to the inclusion and 2 refers to the matrix. The parameter $F$ depends on geometry. For the SCS spheres,

$$F = 4\mu^*/3 \qquad (7)$$

for the effective bulk modulus, $K^*$, and

$$F = \frac{\mu^*(9K^* + 8\mu^*)}{6(K^* + 2\mu^*)} \qquad (8)$$

for the effective shear modulus, $\mu^*$. In the case of the tube-shaped bodies,

$$F = \mu_1/3 + \mu^* \qquad (9)$$

for the effective bulk modulus, $K^*$, and

$$F = 5/\left[\frac{1}{3(K_1 + \mu_1/3 + \mu^*)} + \frac{2(2\mu_1 + \mu^* + g)}{(\mu_1 + \mu^*)(\mu_1 + g)}\right] - \mu_1 \qquad (10)$$

for the effective shear modulus, $\mu^*$, and the parameter, $g$, is given by

$$g = \frac{\mu^*(K^* + \mu^*/3)}{K^* + 7\mu^*/3} \qquad (11)$$

Figure 3 illustrates the results of a typical calculation, in this case for tube-shaped melt bodies (Eqs. (6), (9), (10), and (11)). $(\partial \ln V_S/\partial \ln V_P)_P$ for different melt fractions is calculated from the effective elastic moduli by comparing velocities in regions of partial melt to velocities in unmelted mantle. Elastic properties and densities for the solid fraction are taken from Earth model PREM (Dziewonski and Anderson, 1981). For the melt, the rigidity is zero and the bulk modulus is assumed to be equivalent to that of the solid phase. The viscosity of the melt may be low if low pressure (~1 GPa) results on synthetic silicate liquids which indicate a negative dependence of viscosity on both pressure and volatile content (Dingwell, 1987) also apply at high pressure. However,

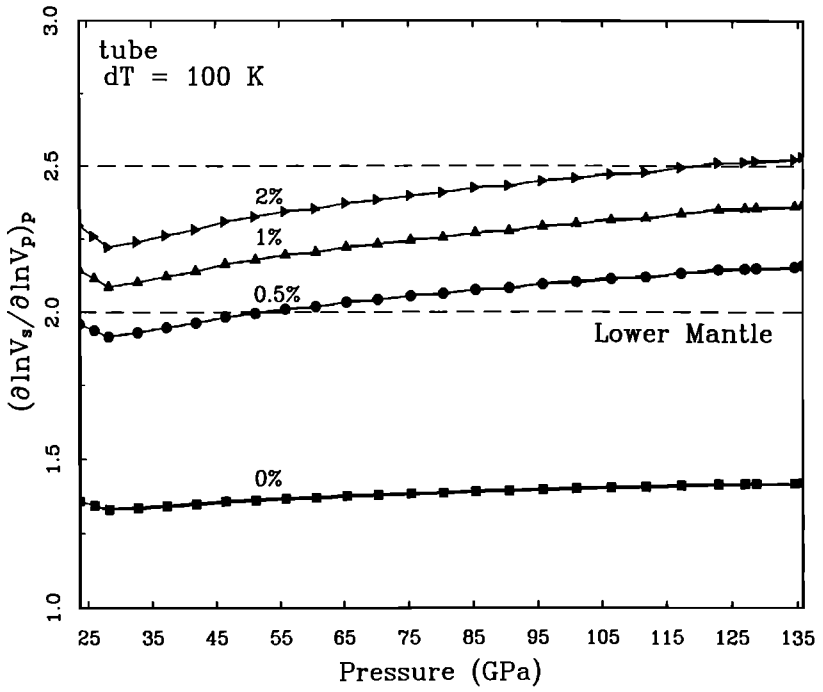


Figure 3. The parameter $(\partial \ln V_S/\partial \ln V_P)_P$ for melt fractions between 0 and 2% at lower mantle pressures. The case shown is for melt distributed in tube-shaped bodies and with a thermal anomaly of 100 K. The bulk modulus of the melt is the same as the residual solid. Dashed lines represent the range of lower mantle values from tomography.

the effect of lower mantle pressures on molten silicate viscosities is uncertain. Theoretical calculations of Angell (1982) indicate that molten silicate viscosities are related to $Si^{+4}$ and $Al^{+3}$ coordination and hence mean interionic distance. As compression occurs to ~30 GPa, oxygen coordination increases tend to increase mean interionic distances. At higher pressure, coordination increases still may occur but the overall compression of the liquid then decreases mean interionic distances and presumably results in a viscosity increase.

The effect of a thermal anomaly on the solid phases must also be taken into account. The magnitude of the thermal effect is obtained using $(\partial V_P/\partial T)_P \approx 0.2$ m/s/K (Duffy and Ahrens, 1991b) and also by assuming $\dot{V}_S = 0.75\dot{V}_P$ from the zero pressure elastic properties of mantle phases (Sumino and Anderson, 1984). For this geometry, melt fractions between 0.5% and 2% satisfy the tomographic results for $(\partial \ln V_S/\partial \ln V_P)_P$. In addition, the combined effects of temperature and melt produce shear velocity anomalies of 0.4% from average and compressional velocity anomalies of 0.2% from average when the thermal anomaly is ~100 K and the melt fraction is 0.5%. If only a thermal anomaly is included (0% melt), the resulting $v$ value is ~1.4.

Calculated sound velocities based on the SCS approach do not agree with measured velocities in sandstones with porosities between 4 and 17% (Dhaliwal and Graham, 1991). This is believed to be due to the inflexibility of the fixed-shape geometries. Walsh (1969) developed a theory in which the liquid phase is a dispersion of randomly oriented penny-shaped inclusions of variable aspect ratio. The self-consistency is removed for computational simplicity, however. The additional degree of freedom (variable aspect ratio) allows the sandstone data to be modeled successfully (Dhaliwal and Graham, 1991). The expressions for the effective bulk and shear moduli for this melt geometry are

$$\frac{K_2}{K^*} = 1 + v_1\left(\frac{K_2 - K_1}{K_2}\right)\frac{3K_2 + 4\mu_1}{3K_1 + 4\mu_1 + g(3K_2 + \mu_2)} \quad (12)$$

$$\frac{\mu_2}{\mu^*} = 1 + \frac{v_1}{5}\left(\frac{\mu_2 - \mu_1}{\mu_2}\right) \cdot \left[1 + \frac{8\mu_2}{4\mu_1 + g(3K_2 + 2\mu_2)}\frac{2(3K_1 + 2\mu_1 + 2\mu_2)}{3K_1 + 4\mu_1 + g(3K_2 + \mu_2)}\right] \quad (13)$$

where 1 refers to the inclusion and 2 refers to the matrix. The parameter $g$ is given by:

$$g = \frac{3\pi\alpha\mu_2}{3K_2 + 4\mu_2} \quad (14)$$

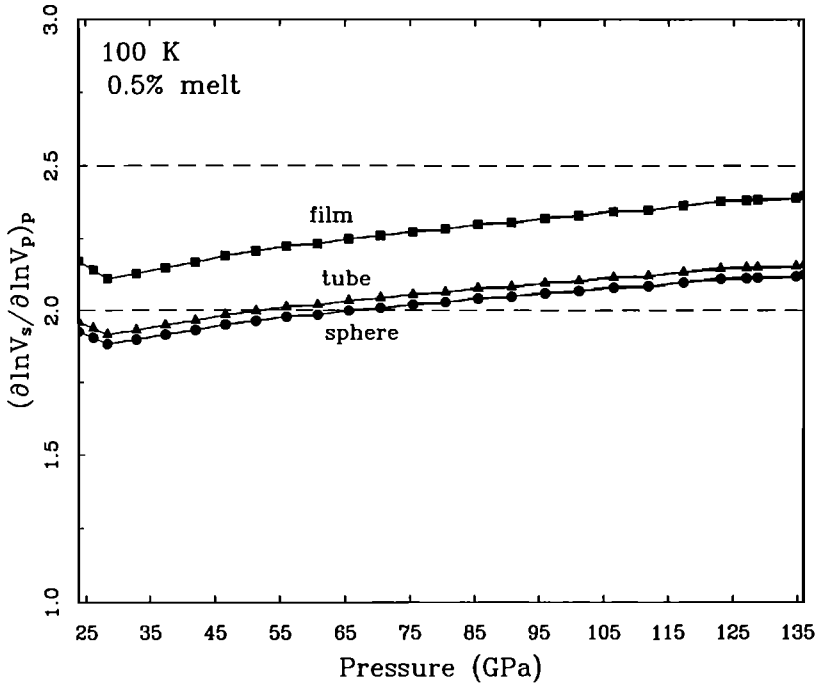


Figure 4. The parameter $(\partial \ln V_S/\partial \ln V_P)_P$ for different melt body geometries at lower mantle pressures. The thermal anomaly is 100 K and the melt fraction is 0.5%. In the case of the film, the aspect ratio is 0.05. Dashed lines represent the range of lower mantle values from tomography.

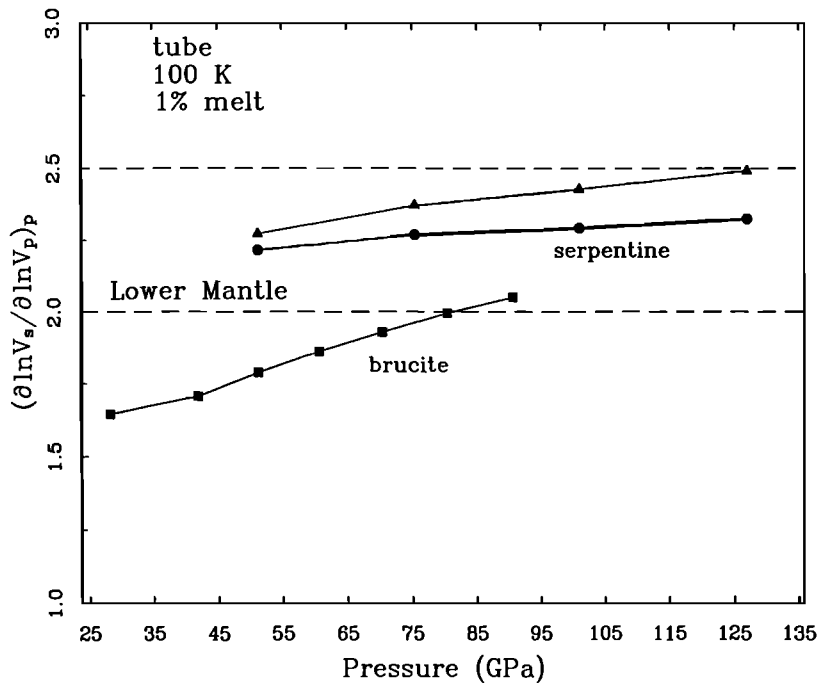


Figure 5. The parameter $(\partial \ln V_S/\partial \ln V_P)_P$ at lower mantle pressures for different melt compressibilities. The solid squares represent the case of melt with the bulk modulus of brucite while the circles and triangles represent the case of melt with the range of bulk moduli of the serpentine high-pressure phase. The bulk moduli of the minerals are from shock wave equation of state data. The melt is distributed in the tube geometry with 1% melt and a 100 K thermal anomaly. Dashed lines represent the range of lower mantle values from tomography.

where $\alpha$ is the aspect ratio of the inclusions.

The effect of geometry on $(\partial \ln V_S/\partial \ln V_P)_P$ for 0.5% melt is shown in Fig. 4. The result for the film (or disk) geometry is calculated using the method of Walsh (1969) (Eqs. (12)–(14)) and an aspect ratio of 0.05. For a given melt fraction, $(\partial \ln V_S/\partial \ln V_P)_P$ is sensitive to the geometric distribution of the melt. In the case of the thin film, $(\partial \ln V_S/\partial \ln V_P)_P$ is strongly dependent on aspect ratio. The melt fraction required to satisfy the tomographically observed $(\partial \ln V_S/\partial \ln V_P)_P$ as well as the magnitude of the anomalies themselves is approximately a factor of 10 larger than the aspect ratio. That is, 0.1% melt is required if the aspect ratio is 0.01 and 0.01% melt is required for an aspect ratio of 0.001. Thus, depending on the geometric distribution of the melt, the melt fraction required to explain the seismic observations may be quite small. Experimental studies have shown that the application of pressure reduces the aspect ratio of cracks in rock specimens (Abdel-Gawad *et al.*, 1987).

The bulk modulus of the melt may differ from the surrounding solid, particularly if it is of different composition (e.g. volatile-rich). To determine the effect of this factor, bulk moduli for the hydrous minerals serpentine and brucite have been determined from shock wave data at lower mantle pressures (Tyburczy *et al.*, 1991; Duffy *et al.*, 1991a). These values were used for the bulk modulus of the melt in the calculation shown in Fig. 5. The bulk modulus of the serpentine high pressure phase is equal to or greater than PREM at a given pressure while $K_S$ for brucite is 40–80% of the PREM values. A lower bulk modulus for the melt phase decreases the value of $v$ while a larger bulk modulus increases its value, for constant $\dot{V}_P$. For the scenario of Fig. 5, $(\partial \ln V_S/\partial \ln V_P)_P$ values within the mantle range occur for melt bulk moduli greater than 0.8 and less than 1.2 times PREM values. Thus, the bulk modulus of the melt must be comparable to that of the surrounding solid in order to satisfy the seismic observations.

## Summary

Values of $(\partial \ln V_S/\partial \ln V_P)_P$ for the lower mantle from seismic tomography can be explained by the presence of variable amounts of hydrous partial melt induced by thermal variations of ~100 K. The amount of partial melt required depends strongly on aspect ratio. For small aspect ratio (0.01–0.001) penny-shaped melt bodies, small melt fractions of 0.01–0.1% can satisfy the seismic observations. For larger aspect ratios or for fixed aspect ratio SCS calculations, the required melt fraction is larger: 0.5–2.0%. These conclusions are similar to those obtained in studies of the upper mantle low velocity zone (Shankland *et al.*, 1981). The bulk modulus of the melt must be comparable to the bulk modulus of the surrounding solid as well.

While partial melting is one possible explanation for these features, other possible explanations exist as discussed above. Furthermore, there is considerable variability in the seismic determinations of $(\partial \ln V_S/\partial \ln V_P)_P$. The existence of water-bearing phases and their state under lower mantle conditions are areas of active study. At present, the two upper bounds on the $H_2O$ content of the lower mantle derivable on the basis of shock devolatilization experiments (0.28% $H_2O$) and from the present $^3He$ flux (0.08% $H_2O$) for the lower mantle are credible. Since initial partial melts of ~1% from such a lower mantle might have 10–25% $H_2O$ contents, the partial melt model with 1–3% melt appears to provide a possible explanation for the value of $v \sim 2$–2.5 observed in the lower mantle. Questions remain about the stability of melts under lower mantle conditions. The issue depends on the density, viscosity, and degree of interconnectedness of the melt. The attenuation of seismic waves by partial melt depends on viscosity and aspect ratio of the melt bodies. A complete model of partial melting must explain the observed $Q$ structure of the lower mantle as well. While these questions cannot be answered at present, the hypothesis that partial melting is responsible for large $(\partial \ln V_S/\partial \ln V_P)_P$ in the lower mantle remains a viable one.

*Acknowledgments.* We appreciate the comments of Don L. Anderson, Robert C. Liebermann, and an anonymous reviewer. The research was supported by NSF and NASA grants. Division of Geological and Planetary Sciences, California Institute of Technology contribution 5042.

## REFERENCES

Abdel-Gawad, M., J Bulau, and B. Tittmann, Qualitative characterization of microcracks at elevated pressure, *J. Geophys. Res.*, *92*, 12911–12916, 1987.

Abe, Y. and T. Matsui, Early evolution of the Earth: Accretion, atmosphere formation and thermal history, *Proc. Lunar Planet. Sci. Conf. 17th, Part 1, J. Geophys. Res., 91, Suppl.*, E291–E302, 1986.

Agnon, A. and M. S. T. Bukowinski, $\delta_S$ at high pressure and $d\ln V_S/d\ln V_P$ in the lower mantle, *Geophys Res. Lett.*, *17*, 1149–1152, 1990.

Ahrens, T. J., Water storage in the mantle, *Nature*, *342*, 122–123, 1989.

Ahrens, T. J., Earth accretion, in *Origin of the Earth*, edited by J. Jones and H. Newson, pp. 211–227, Oxford University Press, New York, 1990.

Allègre, C. J., T. Staudacher, and P. Sarda, Rare gas systematics: formation of the atmosphere, evolution, and structure of the Earth's mantle, *Earth Planet Sci. Lett.*, *81*, 127–150, 1987.

Anders, E. and M. Ebihara, Solar system abundances of the elements, *Geochim. Cosmochim. Acta*, *46*, 2363–2380, 1982.

Anderson, D. L., A seismic equation of state II. shear properties and thermodynamics of the lower mantle, *Phys. Earth Planet. Inter* , *45*, 307–323, 1987.

Anderson, D. L., *Theory of the Earth*, pp. 366, Blackwell, Boston, 1989.

Anderson, D. L. and C. Sammis, Partial melting in the upper mantle, *Phys. Earth Planet. Inter.*, *3*, 41–50, 1970.

Angell, C. A., P. A. Cheeseman, and S. Tamaddon, Pressure enhancement of ion mobilities in liquid silicates from computer simulation studies to 800 kilobars, *Science*, *218*, 885–887, 1982.

Davies, G. F., Earth's neodymium budget and structure and evolution of the mantle, *Nature*, *290*, 208–213, 1981.

Davies, J H., Some problems in mantle structure and dynamics, Ph.D. Thesis, pp. 315, *California Institute of Technology*, Pasadena, CA, 1990.

Dhaliwal, H. and E. K. Graham, A comparison of theoretical rock models with laboratory data, *Tectonophysics*, *188*, 373–383, 1991.

Dingwell, D. B., Melt viscosities in the system $NaAlSi_3O_8$-$H_2O$-$F_2O_{-1}$, in *Magmatic Processes: Physiochemical Principles*, edited by B. O. Mysen, *Geochem. Soc. Spec. Publ. 1*, 423–432, 1987.

Duffy, T. S, T. J. Ahrens, and M. A. Lange, The shock wave equation of state of brucite $Mg(OH)_2$, *J. Geophys. Res.*, *96*, 14319–14330, 1991a.

Duffy, T. S. and T. J. Ahrens, Sound velocities at high pressure and temperature and their geophysical implications, *J Geophys. Res.*, in press, 1991b.

Dziewonski, A. M., Mapping the lower mantle: determination of lateral heterogeneity in P velocity up to degree and order 6, *J. Geophys. Res.*, *89*, 5929–5952, 1984.

Dziewonski, A. D. and D. L. Anderson, Preliminary reference Earth model, *Phys Earth Planet. Inter.*, 25, 297–356, 1981.

Dziewonski, A. M., and J. H. Woodhouse, Global images of the Earth's interior, *Science*, *236*, 37–48, 1987.

Finger, L. W. and C. T. Prewitt, Predicted compositions for high-density hydrous magnesium silicates, *Geophys. Res. Lett.*, *16*, 1395–1397, 1989.

Graham, E. K. and E. G. Hilbert, The effect of pressure on the mantle $d\ln V_S/d\ln V_P$ parameter (abstract), *Eos, Trans AGU*, *69*, 472, 1988.

Green, D. H. and R. C. Liebermann, Phase equilibria and elastic properties of a pyrolite model for the oceanic upper mantle, *Tectonophysics*, *32*, 61–92, 1976.

Hager, B. H. and R. W. Clayton, Constraints on the structure of mantle convection using seismic observations, flow models, and the geoid, in *Mantle Convection: Plate Tectonics and Global Dynamics*, edited by W. R. Peltier, pp. 657–764, Gordon and Breach, New York, 1989.

Inoue, H., Y. Fukao, K. Tanabe, and Y. Ogata, Whole mantle P-wave travel time tomography, *Phys. Earth Planet. Inter.*, *59*, 294–328, 1990.

Isaak, D. G., O. L. Anderson, and T. Goto, Elasticity of single-crystal forsterite measured to 1700 K, *J. Geophys. Res.*, *94*, 5895–5906, 1989.

Ito, E., D. M. Harris, and A. T. Anderson, Alteration of oceanic crust and geologic cycling of chlorine and water, *Geochim. Cosmochim. Acta*, *47*, 1613–1624, 1983.

Jeanloz, R. and S. Morris, Temperature distribution in the crust and mantle, *Ann. Rev. Earth Planet. Sci*, *14*, 377–415, 1986.

Kanzaki, M., Stability of hydrous magnesium silicates in the mantle transition region, *Phys. Earth Planet. Int.*, *66*, 307–312, 1991.

Lange, M. A. and T. J. Ahrens, Impact-induced dehydration of serpentine and the evolution of planetary atmospheres, *Proc. Lunar Planet. Sci. Conf. 13th, Part 1, J. Geophys. Res., Supplement*, *87*, A451–A456, 1982.

Li, X. D., D. Giardini, and J. H. Woodhouse, The relative amplitudes of mantle heterogeneity in P-velocity, S-velocity, and density from free-oscillation data, *Geophys. J.*, *105*, 649–657, 1991.

Li, X. and R. Jeanloz, Phases and electrical conductivity of a hydrous silicate assemblage at lower mantle conditions, *Nature*, *350*, 332–334, 1991.

Liu, L., Effect of $H_2O$ on the phase behavior of the forsterite-enstatite system at high pressures and temperatures and implications for the Earth, *Phys Earth Planet. Inter.*, *49*, 142–167, 1987.

Nataf, H.-C., I. Nakanishi, and D. L. Anderson, Anisotropy and shear-velocity heterogeneities in the upper mantle, *Geophys. Res. Lett.*, *11*, 109–112, 1984.

Nataf, H.-C., I. Nakanishi, and D. L. Anderson, Measurements of mantle wave velocities and inversion for lateral heterogeneities and anisotropy, III. Inversion, *J. Geophys. Res.*, *91*, 7261–7307, 1986.

Peacock, S. M., Fluid processes in subduction zones, *Science*, *248*, 329–337, 1990.

Pulver, S. and T. G. Masters, PCP-P travel times and the ratio of P to S velocity variations in the lower mantle (abstract), *Eos, Trans AGU*, *71*, 1464, 1990.

Reynard, B. and G. D. Price, Thermal expansion of minerals at high pressures—a theoretical study, *Geophys. Res. Lett.*, *17*, 689–692, 1990.

Ringwood, A. E. and A. Major, High-pressure reconnaissance investigations in the system $Mg_2SiO_4$-MgO-$H_2O$, *Earth Planet Sci. Lett.*, *2*, 130–133, 1967.

Ringwood, A. E., *Composition and Petrology of the Earth's Mantle*, 618 pp., McGraw-Hill, New York, 1975.

Romanowicz, B., Seismic tomography of the mantle, *Ann. Rev. Earth and Planet. Sciences*, *19*, 77–100, 1991.

Shankland, T. J., R. J. O'Connell, and H. S. Waff, Geophysical constraints on partial melt in the upper mantle, *Rev. Geophys. Space Phys.*, *19*, 394–406, 1981.

Simmons, G. and H. Wang, Single Crystal Elastic Constants and Calculated Aggregate Properties: A Handbook, 370 pp., MIT Press, Cambridge, MA, 1971.

Sumino, Y., and O. L. Anderson, Elastic constants of minerals, in *Handbook of Physical Properties of Rocks, Vol. III*, edited by R. S. Carmichael, pp. 39–137, CRC Press, Boca Raton, Fla., 1984.

Stevenson, D. J., Models of the Earth's core, *Science*, 611–618, 1981.

Tanimoto, T., Long-wavelength S-wave velocity structure throughout the mantle, *Geophys. J.*, *100*, 327–336, 1990.

Tyburczy, J. A., R. V. Krisnamurthy, S. Epstein, and T. J. Ahrens, Impact-induced devolatilization and hydrogen isotopic fractionation of serpentine—implications for planetary accretion, *Earth Planet. Sci. Lett.*, *98*, 245–260, 1990.

Tyburczy, J. A., T. S. Duffy, and T. J. Ahrens, Shock wave equation of state of serpentine to 150 GPa: Implications for the occurrence of water in the Earth's lower mantle, *J. Geophys. Res.*, in press, 1991.

Walsh, J. B., New analysis of attenuation in partially melted rock, *J. Geophys. Res.*, *74*, 4333–4337, 1969.

Watt, J. P., G. F. Davies, and R. J. O'Connell, The elastic properties of composite materials, *Rev. Geophys. Space Phys.*, *14*, 541–563, 1976.

Welham, T. A. and H. Craig, Methane, hydrogen, and helium in hydrothermal fluids at 21°N on the East Pacific Rise, in *Hydrothermal Processes of Seafloor Spreading Centers*, edited by P. A. Rona, K Bastion, L. Laubier, and K. L. Smith, pp. 391–409, Plenum, New York, 1983.

Wiik, H. B., The chemical composition of some stony meteorites, *Geochim. Cosmochim. Acta*, *9*, 279–289, 1956.

Williams, Q., Molten $(Mg_{0.88}Fe_{0.12})_2SiO_4$ at lower mantle conditions: melting products and structure of quenched glasses, *Geophys. Res. Lett.*, *17*, 635–638, 1990.

Wyllie, P. J., Magma genesis, plate tectonics, and chemical differentiation, in *Rev. Geophys.*, *26*, 370–404, 1988.

Yeganeh-Haeri, A., D. J. Weidner, and E. Ito, Elasticity of $MgSiO_3$ in the perovskite structure, *Science*, *243*, 787–789, 1989.